

## Solid-solid transition of the size-polydisperse hard sphere system

Mingcheng Yang and Hongru Ma

Citation: *The Journal of Chemical Physics* **130**, 031103 (2009); doi: 10.1063/1.3056412

View online: <http://dx.doi.org/10.1063/1.3056412>

View Table of Contents: <http://scitation.aip.org/content/aip/journal/jcp/130/3?ver=pdfcov>

Published by the [AIP Publishing](#)

---

### Articles you may be interested in

[Solid-solid collapse transition in a two dimensional model molecular system](#)

*J. Chem. Phys.* **139**, 194702 (2013); 10.1063/1.4829762

[Solid-solid phase transition in hard ellipsoids](#)

*J. Chem. Phys.* **131**, 164513 (2009); 10.1063/1.3251054

[Solid phase thermodynamic perturbation theory: Test and application to multiple solid phases](#)

*J. Chem. Phys.* **127**, 084512 (2007); 10.1063/1.2756836

[The influence of polytypic structures on the M 011  \$\rightarrow\$  M 101 solid–solid phase transition of n- C 36 H 74 : An application of the oblique infrared transmission method](#)

*J. Chem. Phys.* **121**, 1121 (2004); 10.1063/1.1760072

[A study of the condensed phases and solid–solid phase transition in toluene: A Monte Carlo investigation](#)

*J. Chem. Phys.* **113**, 8070 (2000); 10.1063/1.1316006

---



## Solid-solid transition of the size-polydisperse hard sphere system

Mingcheng Yang and Hongru Ma<sup>a)</sup>

*Institute of Theoretical Physics, Shanghai Jiao Tong University, Shanghai 200240,  
People's Republic of China*

(Received 6 August 2008; accepted 5 November 2008; published online 21 January 2009)

The solid-solid coexistence of a polydisperse hard sphere system is studied by using the Monte Carlo simulation. The results show that for large enough polydispersity the solid-solid coexistence state is more stable than the single-phase solid. The two coexisting solids have different composition distributions but the same crystal structure. Moreover, there is evidence that the solid-solid transition terminates in a critical point as in the case of the fluid-fluid transition. © 2009 American Institute of Physics. [DOI: 10.1063/1.3056412]

The monodisperse hard sphere system is one of the best understood systems in its equilibrium phase behaviors, it undergoes an entropy-driven first-order transition from a disordered fluid to an ordered solid as the volume fraction increases.<sup>1</sup> The system often serves as an excellent starting point to study more complicated systems and a good model for the description of a class of colloidal dispersions. However, in a real colloidal system the particles inevitably exhibit considerable size polydispersity, which influences significantly the thermodynamic and dynamic behaviors of the system.<sup>2–10</sup> Therefore, a more realistic model describing hard sphere colloids is the size-polydisperse hard sphere system. The equilibrium phase behaviors of the polydisperse hard sphere system have not yet been fully understood. Besides the usual fluid-solid transition, a general consensus is that there exists a terminal polydispersity, above which the single-phase crystal becomes thermodynamically unstable. It is not clear what structure is thermodynamically stable when the polydispersity of the crystal exceeds the terminal polydispersity. Some theoretical studies show that beyond the terminal polydispersity the crystal will fractionate into two or more coexisting solid phases with the same crystal structure.<sup>4,5</sup> Others indicate that a crystal-to-glass transition will occur.<sup>11</sup> Experimentally, the crystallization does not occur at large enough polydispersity.<sup>2</sup> From the experiment we draw no definite conclusion about the equilibrium phase behavior because the nonequilibrium effect will dominate the system for such a high polydispersity. So far, the solid-solid coexistence of polydisperse hard sphere system is only a theoretical prediction. In order to confirm the prediction, carefully designed experimental studies and comprehensive computer simulations are needed. To the best of our knowledge, the only simulation evidence up to now comes from the work of Fernández *et al.*<sup>12</sup> In that work they investigated the phase equilibria of the polydisperse soft-sphere system and found that the crystal is highly inhomogeneous at large polydispersity. However, this does not provide us any details about the inhomogeneous structure.

In this paper, we use the Monte Carlo method to investigate the solid-solid transition of a polydisperse hard sphere crystal. To simulate a polydisperse crystal we employ the semigrand ensemble, which is the best frame to study the polydisperse crystal.<sup>3,13,14</sup> In the ensemble the composition distribution is *a priori* unknown, and the independent variables are the chemical potential differences  $\Delta\mu(\sigma)$  of particles of each kind to a reference kind, which are given in advance. As a result, in the ensemble the conditions for coexistence of two phases will be satisfied if only the two phases have the same pressure and referenced chemical potential. As is well known, the first-order transition of a hard sphere system can be identified by looking for a double-peak structure in the volume histogram. Then, by tuning the pressure one can easily detect the transition point where the two peaks have equal weight.<sup>15</sup> In actual computations we locate the transition point using a more tractable criteria “equal peak height,”<sup>16</sup> which differs from equal weight in the finite-size effect and gives the same result in the thermodynamic limit. In the following we describe in detail the simulation method and discuss the obtained results.

In the isobaric semigrand ensemble the quantity  $P_{\text{iso}}(V) = Y(V)\exp(-\beta PV)$  measures the probability density to find a system with the volume  $V$  and the pressure  $P$ , here  $Y(V)$  is the semigrand canonical partition function with given differences of excess chemical potential, defined as

$$Y(V) = \frac{1}{N! \Lambda^{3N}(\sigma_r)} \int_{\sigma_1} \cdots \int_{\sigma_N} Z_N(V) \times \exp \left\{ \beta \sum_{i=1}^N (\mu_{\text{ex}}(\sigma_i) - \mu_{\text{ex}}(\sigma_r)) \right\} \prod_{i=1}^N d\sigma_i, \quad (1)$$

here,  $\sigma_i$  and  $\sigma_r$  are the diameters of the  $i$ th particle and an arbitrarily chosen referenced component, respectively.  $Z_N$  is the canonical configuration integral  $Z_N(V) = \int_V \cdots \int_V e^{-\beta U} \Pi_{i=1}^N d\mathbf{r}_i$  and  $\mu_{\text{ex}}(\sigma_i) = \mu(\sigma_i) - kT \ln(N\Lambda(\sigma_i)^3/V)$  is the excess chemical potential relative to the ideal gas. Once  $Y(V)$  is obtained, the probability density  $P_{\text{iso}}(V)$  can be determined immediately. We now consider the coexistence of two solids having the same structure, in this case the two coexisting solids can be connected with a reversible path as

<sup>a)</sup>Electronic addresses: hrma@sjtu.edu.cn and ymch5010@sjtu.edu.cn.

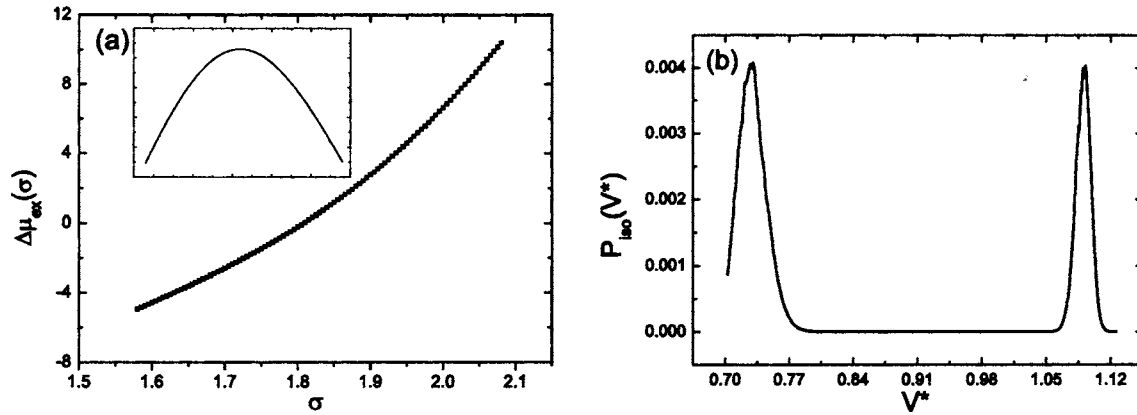


FIG. 1. (a) The chemical potential difference of an initial metastable crystal as a function of the diameter of particles. It is obtained from the SNEPR method. The inset shows the prescribed composition distribution of the metastable crystal. (b) The distribution of the dimensionless volume of the system at the coexisting pressure. It is calculated from the extended ensemble simulation by using the  $\Delta\mu_{\text{ex}}(\sigma)$  plotted in (a).

the coexisting fluids. In order to calculate the  $Y(V)$ , we introduce an extended semigrand canonical ensemble with the volume  $V$  as an additional variable. The partition function of the extended ensemble is defined as

$$\Gamma = \sum_V Y(V, N, T, \Delta\mu_{\text{ex}}(\sigma)), \quad (2)$$

here different volumes correspond to different macroscopic states. By changing the volume the system transforms from one coexisting solid to the other, provided that the solid-solid transition does exist. When we perform a simulation in the extended semigrand canonical ensemble, the probability density of finding the system in volume  $V$  is proportional to  $Y(V, N, T, \Delta\mu_{\text{ex}}(\sigma))$ . So the semigrand canonical partition function  $Y(V, N, T, \Delta\mu_{\text{ex}}(\sigma))$  can be calculated by using the flat histogram methods<sup>17–19</sup> to within an overall multiplier.

Previous calculations<sup>20</sup> show that face-centered-cubic (fcc) phase is still the most stable for the hard sphere crystal with a low size polydispersity. Therefore, both coexisting solids are considered to be the fcc structure. At present, we still have no definite knowledge about the position of polydispersity leading to instability of the single-phase crystal. Specifically, we need a way to find the chemical potential difference function under which the solid-solid transition can occur. Recent studies on the elasticity of the fcc polydisperse hard sphere crystal indicated that there exists a mechanical terminal polydispersity (MTP) above which the crystal is mechanically unstable.<sup>10</sup> The MTP is an upper limit of the thermodynamical terminal polydispersity, thus we expect that a single-phase crystal is in the thermodynamically metastable state at polydispersity slightly below the MTP. Under the chemical potential difference function of the metastable crystal, which can be obtained with the semigrand nonequilibrium potential refinement (SNEPR) algorithm,<sup>20,21</sup> the solid-solid transition may occur. To determine the MTP from elastic constants, a large amount of simulation time is needed. Here, we adopt a simple but effective approach, by which the MTP can be estimated roughly. The approach is based on the observation that, once the polydispersity is higher than the MTP, the SNEPR procedure will converge very slowly or even does not converge. As a result, the MTP can be determined roughly by monitoring the chemical po-

tential difference distribution during the run of the SNEPR algorithm. Once we know the chemical potential difference function of a metastable crystal, we can use it to study the solid-solid transition by calculating the probability densities  $P_{\text{iso}}(V)$ .

We consider four initial metastable crystals with the same composition distribution, but different volume fractions  $\eta=0.59, 0.583, 0.576,$  and  $0.566$ . Correspondingly, we have four different chemical potential difference functions. Here, we emphasize that in the simulation we do not try to fix the parent composition and to determine the cloud point. The only reason for choosing the initial metastable crystals is that under their chemical potential difference distribution, the solid-solid transition can occur. The composition of the initial metastable crystal is a truncated Schulz function. The criteria of the truncation is that the probability densities at both ends of the distribution are equal, and they are about three-fifths of the maximum probability density, as shown in inset of Fig. 1(a). In present work the effect of the truncation is not studied, however, the cutoff is necessary for the following reasons. First, the particles of small size may enter into the interstitial space of crystals, which will induce the point defect in the crystal. Second, the difference of the composition between two coexisting solids is quite large except for the critical region (see Fig. 3), hence, the sampling of the large particle is very poor in the lower density coexisting solid. All the simulations are performed with a system of 256 size-polydisperse hard spheres in a parallelepiped box; periodic boundary conditions are used in all three directions. Figures 1(a) and 2(a) are two typical chemical potential difference functions of the initial metastable crystals. They are obtained by applying the SNEPR method to the initial crystals. The initial crystal in Fig. 1 has higher volume fraction than the one in Fig. 2, so its chemical potential difference is larger. Figures 1(b) and 2(b) show the distributions of the dimensionless volume of the system, which are calculated from the extended semigrand canonical ensemble simulation by using the solved chemical potential difference functions plotted in Figs. 1(a) and 2(a), respectively. The dimensionless volume is defined as  $V^*=V/N(\bar{\sigma})^3$ , here  $\bar{\sigma}$  is the average of the diameter of particles of the initial metastable crystal.

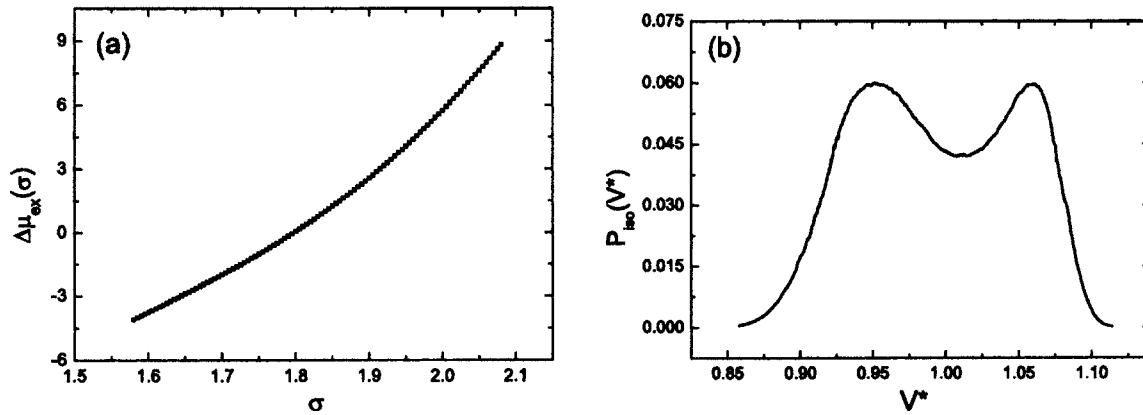


FIG. 2. The same as Fig. 1, the volume fraction of the initial metastable crystal is less than that in Fig. 1.

The distributions clearly exhibit a double-peak structure for a range of pressure, which is the sign of the solid-solid transition. At the coexisting pressure the two peaks have equal height, each peak represents a coexisting solid, and the volumes of two coexisting solids are determined from the positions of the peak maximum. The composition distribution of each coexisting solid can be obtained from an additional semigrand canonical simulation by the same chemical potential difference function. Figure 3 displays the particle size distributions of the coexisting solids. The compositions of two coexisting solids are significantly different, i.e., the fractionation effect is sufficiently large. The coexisting solid with lower volume fraction has a larger polydispersity than the one with higher volume fraction, which is consistent with the results by Fasolo and Sollich.<sup>5</sup> The composition of the coexisting solids looks a little bit unnatural due to the truncation, however, the cutoff of the size distribution will not qualitatively influence the existence of the solid-solid transition. In the simulation we find that the separation between the two peaks decreases as the volume fraction of initial solid decreases, as shown in Figs. 1(b) and 2(b). We expect that the two peaks will completely merge together under some special conditions. This gives the solid-solid critical point, sketched by the filled circle in Fig. 4. The early studies also indicated that a monodisperse system of hard spheres with a short-ranged attractive interaction undergoes a solid-solid

transition with the same crystal structure and has a solid-solid critical point.<sup>22,23</sup> We argue that the critical phenomena of the polydisperse crystal is not experimentally observable, since in a real colloidal crystal the particles are not permitted to exchange their positions and to change their sizes.

Figure 4 shows the coexisting solids plotted in the polydispersity and volume fraction plane. Even though we do not determine the cloud points (the estimate of cloud points needs more simulation time and techniques<sup>24</sup>), from the figure we can draw some important conclusions. For the systems under consideration we note that, except the lower density solid in Fig. 3(b) (the uppermost triangle in Fig. 4), the coexisting phases with lower volume fraction have similar size distribution function and follow a linear relation. So the linear fit roughly resembles a cloud curve (dashed line). On the right side of the cloud curve the single-phase solid becomes thermodynamically unstable. The cloud curve has a negative slope, so for each volume fraction of interest there exists a maximum polydispersity, above which the solid-solid coexistence occurs. On the other hand, all the coexisting solids with higher volume fraction also have the similar size distribution. Thus we get a second approximate cloud curve by a linear fitting (dotted line). Comparing with the first case, the unstable region lies on the left side of the cloud curve, and for each volume fraction under consideration there exists a minimum polydispersity stabilizing a single-

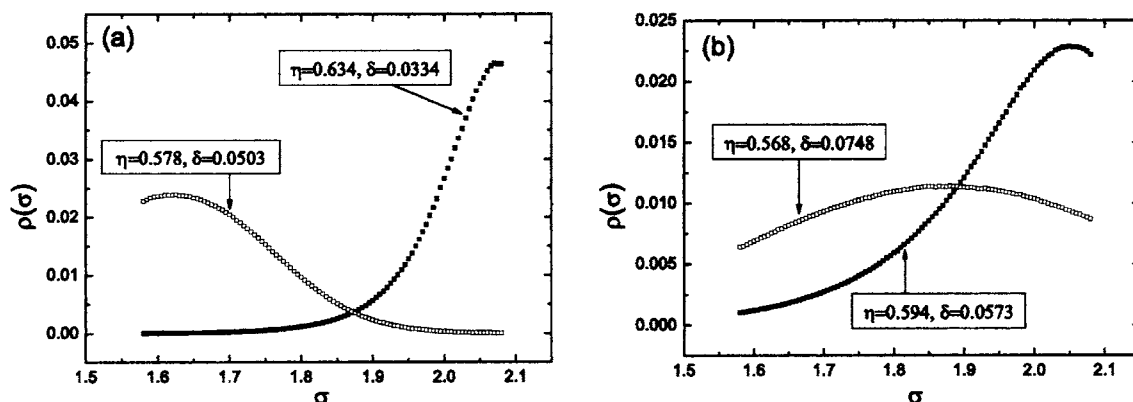


FIG. 3. (a) The composition distribution of the coexisting solids given in Fig. 1(b). The solids with the lower (open square) and higher (filled square) volume fractions correspond to the left and right peaks in Fig. 1(b), respectively. This is because the large volume accommodates easily the larger particles. Here,  $\eta$  is the volume fraction and  $\delta$  is the polydispersity. (b) The composition distribution of the coexisting solids given in Fig. 2(b).



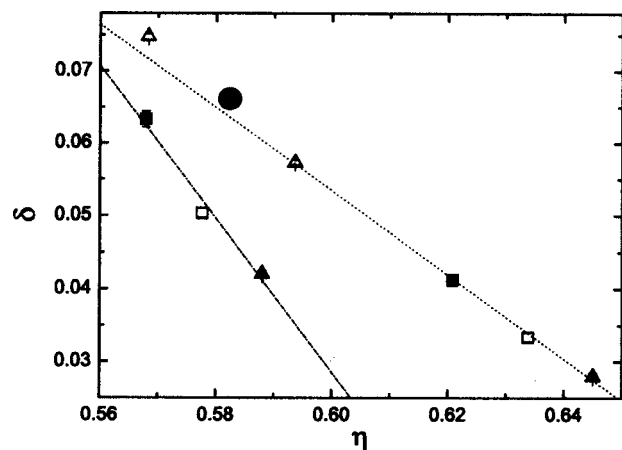


FIG. 4. The solid-solid coexistence plotted in volume fraction  $\eta$  and polydispersity  $\delta$  plane. The symbols of the same type denote the two coexisting solids with the same chemical potential difference distribution, which is obtained by applying the SNEPR method to the initial metastable crystal and from bottom to top different symbols correspond to the initial metastable crystals with different volume fractions,  $\eta=0.59$ ,  $0.583$ ,  $0.576$ , and  $0.566$ , respectively. Here, the tie-curve connecting the two coexisting phases is not plotted. Dashed line is a linear fit for the coexisting solids with the lower volume fraction except the uppermost triangle. [For the size distribution function of the coexisting crystal denoted by the uppermost triangle is remarkably different from other lower density coexisting crystals. It should be noted that the polydispersity of the uppermost triangle is still under the MTP. Because our previous study (Ref. 10) showed that the MTP of the polydisperse hard sphere crystal with Schulz distribution is about  $0.081$ , which is higher than that of the uppermost triangle with Schulz-type distribution presented in Fig. 3(b)]. Dotted line is a linear fit for the coexisting solids with the higher volume fraction; the filled circle gives a guess for the critical point.

phase solid. Because the monodisperse crystal is stable in the volume fraction range of the simulation, the cloud curve will bend back at the lower polydispersity, where the fluid-solid transition occurs. However, with further increasing the polydispersity the cloud curve will bend back toward the high volume fraction due to the existence of the terminal polydispersity. The cloud curve looks like a “reverse-Z.” Under some chemical potential distribution both the fluid-solid and solid-solid transitions can occur. Usually, in the fluid-solid transition the coexisting solid with a smaller volume contains larger particles. However, for the solid-solid coexistence under consideration, the coexisting solid with a larger volume contains larger particles (see the caption of Fig. 3). As a result, on the volume axis the region of the fluid-solid coexistence is separated from the solid-solid coexistence region by the solid with majority larger particles (i.e., the two coexistence regions do not overlap). Therefore, the solid-solid transition is stable with respect to melting. Under some special condition, the coexistence of two solids with a fluid phase and even the metastable solid-solid coexistence are also possible.

In summary, we investigated the solid-solid transition of the size-polydisperse hard sphere system by the Monte Carlo simulation. The results indicate that at sufficient high polydispersity the single-phase solid becomes unstable and the solid-solid coexistence will occur. Two coexisting solid phases have different composition distributions. We also find that the solid-solid critical point can exist under some special conditions. Although we do not calculate the cloud points, we can obtain some qualitative understanding about the solid-solid phase diagram. It is possible to calculate the cloud points in the current frame.<sup>24</sup> The existence of the solid-solid coexistence state cannot preclude the occurrence of the glass transition, but we prefer to think of the glass transition as a kinetic phenomenon.

The work is supported by the National Natural Science Foundation of China under Grant Nos. 10874111 and 10334020 and in part by the National Minister of Education Program for Changjiang Scholars and Innovative Research Team in University.

- <sup>1</sup>W. G. Hoover and F. H. Ree, *J. Chem. Phys.* **49**, 3609 (1968).
- <sup>2</sup>P. N. Pusey and W. van Meegen, *Nature (London)* **320**, 340 (1986).
- <sup>3</sup>P. G. Bolhuis and D. A. Kofke, *Phys. Rev. E* **54**, 634 (1996); D. A. Kofke and P. G. Bolhuis, *ibid.* **59**, 618 (1999).
- <sup>4</sup>P. Bartlett, *J. Chem. Phys.* **109**, 10970 (1998).
- <sup>5</sup>M. Fasolo and P. Sollich, *Phys. Rev. Lett.* **91**, 068301 (2003).
- <sup>6</sup>S. Phan, W. B. Russel, Z. Cheng, J. Zhu, P. M. Chaikin, J. H. Dunsmuir, and R. H. Ottewill, *Phys. Rev. E* **54**, 6633 (1996).
- <sup>7</sup>S. Phan, W. B. Russel, J. Zhu, and P. M. Chaikin, *J. Chem. Phys.* **108**, 9789 (1998).
- <sup>8</sup>S. Martin, G. Bryant, and W. van Meegen, *Phys. Rev. E* **67**, 061405 (2003).
- <sup>9</sup>H. J. Schope, G. Bryant, and W. van Meegen, *Phys. Rev. Lett.* **96**, 175701 (2006).
- <sup>10</sup>M. C. Yang and H. R. Ma, *Phys. Rev. E* **78**, 011404 (2008).
- <sup>11</sup>P. Chaudhuri, S. Karmakar, C. Dasgupta, H. R. Krishnamurthy, and A. K. Sood, *Phys. Rev. Lett.* **95**, 248301 (2005).
- <sup>12</sup>L. A. Fernández, V. Martín-Mayor, and P. Verrocchio, *Phys. Rev. Lett.* **98**, 085702 (2007).
- <sup>13</sup>D. A. Kofke and E. D. Glandt, *J. Chem. Phys.* **87**, 4881 (1987).
- <sup>14</sup>M. A. Bates and D. Frenkel, *J. Chem. Phys.* **109**, 6193 (1998).
- <sup>15</sup>C. Borgs and R. Kotecký, *J. Stat. Phys.* **61**, 79 (1990); *Phys. Rev. Lett.* **68**, 1734 (1992).
- <sup>16</sup>M. S. S. Challa, D. P. Landau, and K. Binder, *Phys. Rev. B* **34**, 1841 (1986).
- <sup>17</sup>B. A. Berg and T. Neuhaus, *Phys. Rev. Lett.* **68**, 9 (1992).
- <sup>18</sup>F. Wang and D. P. Landau, *Phys. Rev. Lett.* **86**, 2050 (2001); *Phys. Rev. E* **64**, 056101 (2001).
- <sup>19</sup>J. S. Wang and R. H. Swendsen, *J. Stat. Phys.* **106**, 245 (2002).
- <sup>20</sup>M. C. Yang and H. R. Ma, *J. Chem. Phys.* **128**, 134510 (2008).
- <sup>21</sup>N. B. Wilding, *J. Chem. Phys.* **119**, 12163 (2003).
- <sup>22</sup>P. G. Bolhuis and D. Frenkel, *Phys. Rev. Lett.* **72**, 2211 (1994).
- <sup>23</sup>C. F. Tejero, A. Daanoun, H. N. W. Lekkerkerker, and M. Baus, *Phys. Rev. Lett.* **73**, 752 (1994).
- <sup>24</sup>M. Buzzacchi, P. Sollich, N. B. Wilding, and M. Müller, *Phys. Rev. E* **73**, 046110 (2006).